RESEARCH ARTICLE

Defining the Roles of TcdA and TcdB in Localized Gastrointestinal Disease, Systemic Organ Damage, and the Host Response during *Clostridium difficile* Infections

Glen P. Carter,[a] Anjana Chakravorty,[a] Tu Anh Pham Nguyen,[b] Steven Mileto,[a] Fernanda Schreiber,[b] Lucy Li,[a] Pauline Howarth,[a] Simon Clare,[b] Bliss Cunningham,[a] Susan P. Sambol,[c,d] Adam Cheknis,[c,d] Iris Figueroa,[c,d] Stuart Johnson,[c,d] Dale Gerding,[c,d] Julian I. Rood,[a] Gordon Dougan,[b] Trevor D. Lawley,[b] Dena Lyras[a]

Department of Microbiology, Monash University, Victoria, Australia[a]; Wellcome Trust Sanger Institute, Hinxton, United Kingdom[b]; Medical Service and Research Service, Hines VA Hospital, Hines, Illinois, USA[c]; Infectious Disease Section, Stritch School of Medicine, Loyola University Chicago, Maywood, Illinois, USA[d]

G.P.C. and A.C. contributed equally to the work.

ABSTRACT ***Clostridium difficile* is a leading cause of antibiotic-associated diarrhea, a significant animal pathogen, and a worldwide public health burden. Most disease-causing strains secrete two exotoxins, TcdA and TcdB, which are considered to be the primary virulence factors. Understanding the role that these toxins play in disease is essential for the rational design of urgently needed new therapeutics. However, their relative contributions to disease remain contentious. Using three different animal models, we show that TcdA$^+$ TcdB$^-$ mutants are attenuated in virulence in comparison to the wild-type (TcdA$^+$ TcdB$^+$) strain, whereas TcdA$^-$ TcdB$^+$ mutants are fully virulent. We also show for the first time that TcdB alone is associated with both severe localized intestinal damage and systemic organ damage, suggesting that this toxin might be responsible for the onset of multiple organ dysfunction syndrome (MODS), a poorly characterized but often fatal complication of *C. difficile* infection (CDI). Finally, we show that TcdB is the primary factor responsible for inducing the *in vivo* host innate immune and inflammatory responses. Surprisingly, the animal infection model used was found to profoundly influence disease outcomes, a finding which has important ramifications for the validation of new therapeutics and future disease pathogenesis studies. Overall, our results show unequivocally that TcdB is the major virulence factor of *C. difficile* and provide new insights into the host response to *C. difficile* during infection. The results also highlight the critical nature of using appropriate and, when possible, multiple animal infection models when studying bacterial virulence mechanisms.**

IMPORTANCE ***Clostridium difficile* is a leading cause of antibiotic-associated diarrhea and an important hospital pathogen. TcdA and TcdB are thought to be the primary virulence factors responsible for disease symptoms of *C. difficile* infections (CDI). However, the individual contributions of these toxins to disease remain contentious. Using three different animal models of infection, we show for the first time that TcdB alone causes severe damage to the gut, as well as systemic organ damage, suggesting that this toxin might be responsible for MODS, a serious but poorly understood complication of CDI. These findings provide important new insights into the host response to *C. difficile* during infection and should guide the rational development of urgently required nonantibiotic therapeutics for the treatment of CDI.**

Received 27 April 2015 **Accepted** 6 May 2015 **Published** 2 June 2015

Citation Carter GP, Chakravorty A, Pham Nguyen TA, Mileto S, Schreiber F, Li L, Howarth P, Clare S, Cunningham B, Sambol SP, Cheknis A, Figueroa I, Johnson S, Gerding D, Rood JI, Dougan G, Lawley TD, Lyras D. 2015. Defining the roles of TcdA and TcdB in localized gastrointestinal disease, systemic organ damage, and the host response during *Clostridium difficile* infections. mBio 6(3):e00551-15. doi:10.1128/mBio.00551-15.

Invited Editor Jimmy D. Ballard, University of Oklahoma Health Sciences Center **Editor** R. John Collier, Harvard Medical School

Address correspondence to Dena Lyras, Dena.Lyras@monash.edu.

Hospital-acquired infection with the Gram-positive, spore-forming bacterium *Clostridium difficile* is a major global public and veterinary health concern. This pathogen causes severe gastrointestinal illness and death and is the most significant cause of hospital-acquired diarrhea in many countries, which places a considerable economic burden on health care systems (1). The importance of *C. difficile* occurrence in animals has also recently become apparent, with disease or carriage identified in domestic animals, including pigs, cattle, horses, and companion animals (2, 3). *C. difficile* causes a spectrum of gastrointestinal diseases, collectively known as *C. difficile* infections (CDI), which can range from mild diarrhea through moderately serious disease to severe pseudomembranous colitis (1). Unlike the case for other enteric pathogens, disease is almost always associated with antimicrobial therapy. Importantly, the increase in antibiotic-resistant so-called "superbugs" in recent years has led to much higher usage of broad-spectrum antibiotics. Paradoxically, treating these superbugs has left patients vulnerable to infection by opportunistic pathogens, such as *C. difficile*.

After infection is established, most *C. difficile* strains produce two major toxins, TcdA and TcdB, which are encoded by the *tcdA* and *tcdB* genes and are both members of the large clostridial cy-

totoxin family. These toxins are potent monoglucosyltransferases that irreversibly modify members of the Rho family of host regulatory proteins, leading to disruption of downstream signaling pathways and cell death (4). Infection with toxigenic *C. difficile* strains therefore causes extensive colonic inflammation and epithelial tissue damage. The net effect is rapid fluid loss into the intestinal lumen, which manifests as diarrhea (4). *C. difficile* isolates that produce TcdB but not TcdA have emerged and continue to be isolated; these isolates cause the full clinical spectrum of CDI despite only producing one of the major toxins (5). Many human and animal strains also produce a third toxin, binary toxin or CDT, encoded by the *cdtA* and *cdtB* genes (6). The role of this toxin during infection and disease remains to be elucidated; however, recent studies suggest that this toxin may play a role in adherence and colonization of *C. difficile* in the host (6).

In the absence of methods to genetically manipulate *C. difficile*, early disease studies involved the intragastric administration of purified toxins to animals. This research suggested that TcdA was the major virulence factor and that TcdB played a less important role in disease (7). This hypothesis was challenged upon the emergence of naturally occurring variant strains that did not produce TcdA but did produce TcdB (TcdA$^-$ TcdB$^+$) that caused fulminant human CDI (5). Two recent infection studies in hamsters attempted to clarify the roles of TcdA and TcdB in disease by using isogenic toxin mutants constructed in the low-virulence clinical isolate 630 (8, 9). The first study found that TcdB alone resulted in disease (9), while the second concluded that both TcdB and TcdA could individually cause severe disease (8). More recently, a third study using isogenic mutants constructed in strain R20291, an epidemic BI/NAP1/027 strain, together with a hamster infection model also concluded that both toxins could cause fulminant disease independently (10). A number of possibilities could explain the discrepancies in the first two studies, such as genetic differences in the *C. difficile* 630-derived strains, differences in animal challenge protocols, or variations in the intestinal microbiota of animals at different research facilities, which can substantially influence infection outcomes (11). As a consequence, it was suggested that the same panel of strains should be virulence tested in multiple laboratories to minimize the impact of experimental variation (12). To address these disparities and comprehensively define the contributions of TcdA and TcdB to disease, we used three independent animal models to study the relative virulence of a new group of isogenic *C. difficile* toxin gene mutants derived from a Canadian epidemic *C. difficile* BI/NAP1/027 isolate (strain M7404) that had not been extensively laboratory passaged.

RESULTS

Construction and characterization of *tcdA*, *tcdB*, and *cdtA* toxin gene mutants in a BI/NAP1/027 clinical isolate. Two independent *tcdA* (TcdA$^-$ TcdB$^+$) and *tcdB* (TcdA$^+$ TcdB$^-$) mutants (mutants 1 and 2 for each) and a *tcdAB* (TcdA$^-$ TcdB$^-$) double mutant were constructed in strain M7404. Like all BI/NAP1/027 isolates, this strain encodes a third toxin, CDT, an ADP-ribosyltransferase binary toxin (13), which was disrupted separately by mutagenesis of the *cdtA* gene (CDT$^-$). Before virulence testing, each mutant was genotypically confirmed by PCR (data not shown) and Southern hybridization analysis, which confirmed the specific targetron insertions (see Fig. S1 in the supplemental material). Western immunoblot analyses (see Fig. S2) together with Vero and HT29 cell cytotoxicity and neutralization assays (see Fig. S3 and S4) then confirmed the expected toxin profile of each mutant compared to that of the wild type. No differences in the sporulation frequencies of the mutant and wild-type strains were detected (see Table S1).

TcdB-producing strains are more virulent than *tcdB*-deficient isogenic mutants in mouse and hamster infection models. To maximize the robustness of the infection outcomes, we used three different animal models, performed in three independent laboratories. First, an optimized mouse infection model, based on a previously published model (14) and further developed at Monash University (Australia), in which animals consistently develop severe disease was used. Infection with the wild type (TcdA$^+$ TcdB$^+$) and the TcdA$^-$ TcdB$^+$ mutants resulted in marked weight loss (Fig. 1A), with 100% and 95% of mice, respectively, dying within 48 h, rising to 100% for the latter group by 72 h (Fig. 1B). These animals also showed other signs of severe disease, such as shallow and labored breathing, profuse diarrhea, and isolation from littermates (Fig. 1C). In contrast, only moderate weight loss was recorded for TcdA$^+$ TcdB$^-$ strain-infected mice (Fig. 1A); significantly more (80%) of these animals survived than did wild-type strain-infected animals (log rank test, $P < 0.0001$) (Fig. 1B), and they showed significantly less signs of physiological distress (Mann-Whitney test, $P < 0.001$) (Fig. 1C). Importantly, a 500-fold-higher infectious dose of the TcdA$^+$ TcdB$^-$ strain did not elicit more severe disease outcomes (see Fig. S5A and B in the supplemental material) than the lower dose (Fig. 1A and B). Finally, TcdA$^-$ TcdB$^-$ strain-infected mice lost no weight (Fig. 1A), survived the infection (Fig. 1B), and exhibited no other disease signs (Fig. 1C). As with the TcdA$^+$ TcdB$^-$ strain-infected mice, the results for survival and physiological distress were significantly different in TcdA$^-$ TcdB$^-$ strain-infected mice than in mice infected with the wild-type strain ($P < 0.0001$ for both survival and distress). Statistical analysis using a Mann-Whitney test subsequently showed that mice infected with TcdB-producing strains had significantly shorter colons than mock-infected mice ($P < 0.0001$ for the wild-type strain, $P = 0.004$ and $P < 0.001$ for TcdA$^-$ TcdB$^+$ mutants 1 and 2, and $P < 0.001$ and $P < 0.001$ for CDT$^-$ mutants 1 and 2) (Fig. 1D), a common feature in mouse models of ulcerative colitis (15). The colon lengths in the TcdA$^+$ TcdB$^-$ ($P = 0.345$ and $P = 0.540$) and TcdA$^-$ TcdB$^-$ ($P = 0.862$) strain-infected mice were statistically the same as in mock-infected mice (Fig. 1D).

Disease resulting from infection with the CDT$^-$ mutants was indistinguishable from disease caused by the wild type for each parameter analyzed (Fig. 1A to D). Note that in all subsequent animal infection experiments, only one TcdA$^-$ TcdB$^+$, TcdA$^+$ TcdB$^-$, or CDT$^-$ mutant was assessed since the infection phenotypes between the independent mutants using the Monash model were identical.

Strain virulence was next tested at the Sanger Institute (United Kingdom), using a different mouse infection model in which animals typically develop self-limiting intestinal inflammation and rarely progress to severe disease or death (16). Unexpectedly, 40% of TcdA$^-$ TcdB$^+$ strain-infected mice succumbed to acute infection within 48 h, which was a significantly higher rate than for mice infected with the wild-type strain (log rank test, $P = 0.015$) (Fig. 1E). In contrast, animals infected with the wild-type, TcdA$^+$ TcdB$^-$, TcdA$^-$ TcdB$^-$, or CDT$^-$ strain all survived the infection (Fig. 1E).

Finally, the hamster model of CDI developed at Hines VA Hos-

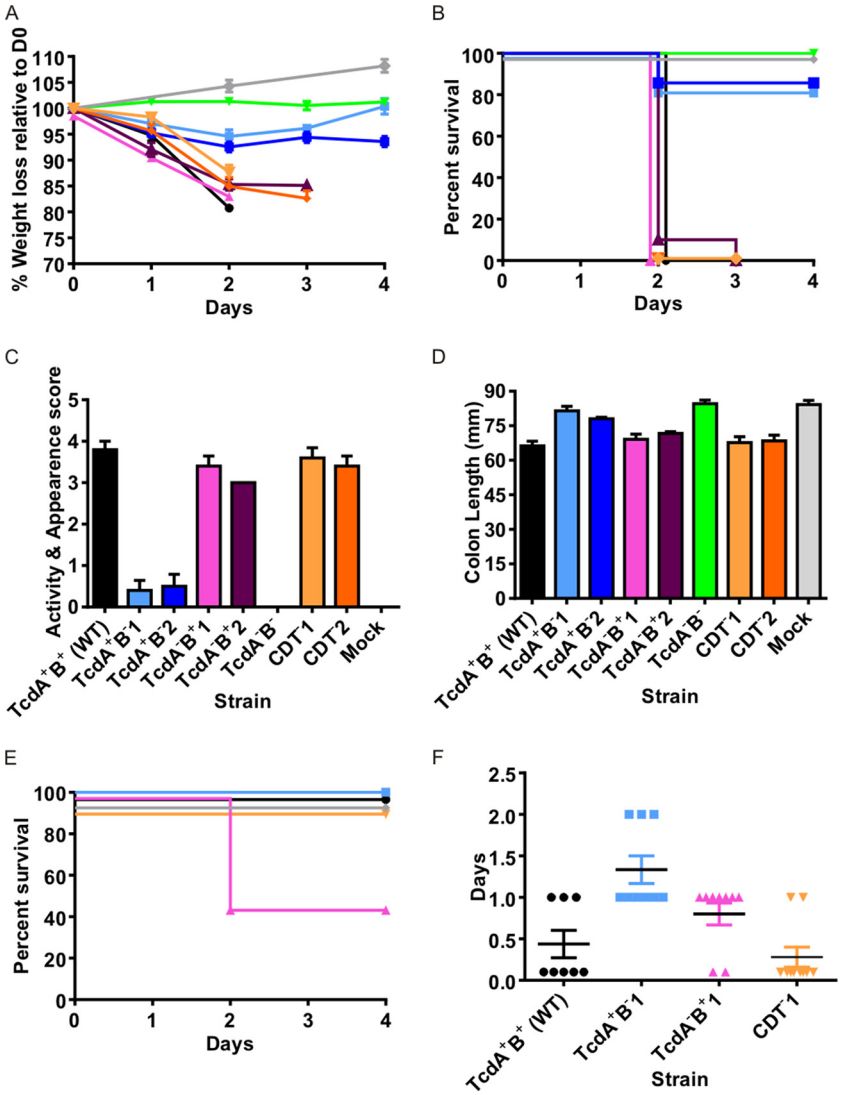

FIG 1 Toxin B is the primary mediator of fulminant *C. difficile* disease. (A to D) Monash mice were infected with *C. difficile* strains. Results for the strains are indicated by different colors as follows: black, wild-type strain M7404 [TcdA$^+$B$^+$ (WT)] (n = 19); light blue, *tcdB* mutant 1 (TcdA$^+$B$^-$1) (n = 14); dark blue, *tcdB* mutant 2 (TcdA$^+$B$^-$2) (n = 10); pink, *tcdA* mutant 1 (TcdA$^-$B$^+$1) (n = 13); purple, *tcdA* mutant 2 (TcdA$^-$B$^+$2) (n = 10); green, *tcdA tcdB* double mutant (TcdA$^-$B$^-$) (n = 15); light orange, *cdtA* mutant 1 (CDT$^-$1) (n = 10); dark orange, *cdtA* mutant 2 (CDT$^-$2) (n = 10); and gray, mock-infected control (mock) (n = 5). Results are shown for weight loss (A), survival (B), activity and appearance (C), and colon length (D) of infected Monash mice. (E) Survival of Sanger mice infected with *C. difficile* strains indicated by different colors as follows: black, wild-type TcdA$^+$ TcdB$^+$ strain [TcdA$^+$B$^+$ (WT)] (n = 16); light blue, TcdA$^+$ TcdB$^-$ mutant 1 (TcdA$^+$B$^-$1) (n = 16); pink, TcdA$^-$ TcdB$^+$ mutant 1 (TcdA$^-$B$^+$1) (n = 13); light orange, *cdtA* mutant 1 (CDT$^-$1) (n = 15); and gray, mock infected (n = 15). (F) Days from infection to death of Hines hamsters infected with *C. difficile* strains indicated by different colors as follows: black, wild-type TcdA$^+$ TcdB$^+$ strain [TcdA$^+$B$^+$ (WT)] (n = 8); light blue, TcdA$^+$ TcdB$^-$ mutant 1 (TcdA$^+$B$^-$1) (n = 9); pink, TcdA$^-$ TcdB$^+$ mutant 1 (TcdA$^-$B$^+$1) (n = 9); and light orange, *cdtA* mutant 1 (CDT$^-$1) (n = 10). Data represent the mean results ± standard deviations (SD).

pital and used in earlier studies (9) was used here. In contrast to the mouse infection results, all infected hamsters died irrespective of the infecting strain (Fig. 1F). However, a significant delay (log rank test, $P = 0.0015$) was evident in the time from colonization to death of TcdA$^+$ TcdB$^-$ strain-infected animals (1.33 ± 0.16 days [mean ± standard deviation]) compared to the time to death for wild-type strain-infected animals (0.43 ± 0.16 days). There was no statistical difference in the time to death of TcdA$^-$ TcdB$^+$ (0.8 ± 0.13 days) or CDT$^-$ (0.28 ± 0.12 days) strain-infected animals compared to the time to death of wild-type strain-infected animals (Fig. 1F). These results indicate that in the hamster model of infection, only the TcdA$^+$ TcdB$^-$ mutant was attenuated in virulence, which agreed with our previous data using toxin mutants in *C. difficile* strain 630 (9).

To ensure that each strain used in this analysis germinated and colonized the infected hosts with equal efficiency, the colonization efficiencies of the *tcdA* (TcdA$^-$ TcdB$^+$ mutant 1) and *tcdB* (TcdA$^+$ TcdB$^-$ mutant 1) mutants in comparison to that of the wild-type M7404 TcdA$^+$ TcdB$^+$ strain in the Monash mouse model of CDI and the Hines VA Hospital hamster infection model were determined. No differences were seen in either mice or hamsters, confirming that such differences were not responsible for disease attenuation resulting from infection with the TcdA$^+$ TcdB$^-$ mutants (see Fig. S6A and D in the supplemental material).

Competition assays were also performed in which Monash mice were simultaneously infected with equal numbers of the *tcdA* (TcdA$^-$ TcdB$^+$ mutant 1) and *tcdB* (TcdA$^+$ TcdB$^-$ mutant 1) mutants to determine whether either strain was reduced in fitness *in vivo* (see Fig. S6E). As expected, both strains were found to be equally fit *in vivo*, with competitive index (CI) values of 1.178 ± 0.267 and 1.119 ± 0.361 obtained at 24 h and 48 h after infection, respectively. This result confirms that the attenuated virulence of the TcdA$^+$ TcdB$^-$ mutants is not due to reduced *in vivo* fitness of these strains. Finally, to confirm that the toxin levels produced by the mutant strains were equivalent to those produced by the wild-type strain *in vivo*, TcdA- and TcdB-specific cytotoxicity assays were performed on the luminal contents of mice infected with each strain (see Fig. S6B and C). Each strain was found to produce the expected toxin *in vivo*, at levels that were not significantly different from the levels detected from the wild-type strain.

Infection with TcdB-producing strains causes severe gut and distal organ damage. Previous studies assessing the roles of TcdA and TcdB in disease did not investigate histological damage arising in the gut as a consequence of CDI. Here, the microscopic effects of TcdA, TcdB, and CDT on the gut—in colonic and cecal tissues from Monash mice and cecal tissues from Sanger mice, collected 2 and 4 days postinfection, respectively—were examined by histopathology. Similar observations were made for both groups, with the wild type and the TcdA$^-$ TcdB$^+$ mutants all causing severe gut damage associated with eroded and often absent crypts, mucosal ulceration, and goblet cell loss (Fig. 2A). Polymorphonuclear cell (PMN) influx into the lamina propria, enterocyte hyperplasia, and severe submucosal edema associated with hemorrhage were also seen (Fig. 2A). In contrast, TcdB-negative strains caused limited tissue damage that was confined to mild edema and PMN influx (Fig. 2A), even when a 500-fold increased dose of the TcdA$^+$ TcdB$^-$ strain relative to the dose of the wild type was used (see Fig. S5C to E in the supplemental material). All of the damage was TcdB- or TcdA-induced, since tissues from TcdA$^-$ TcdB$^-$ strain-infected mice resembled those from mock-infected control mice (Fig. 2A). Independent histological scoring confirmed these observations, with TcdB-producing strains eliciting the greatest injury and strains only producing TcdA causing less damage (Fig. 2B and C). Statistical analysis using a Mann-Whitney test showed significantly less intestinal damage than in wild-type strain-infected mice only in animals infected with the TcdA$^+$ TcdB$^-$ mutants ($P = 0.0022$ and $P = 0.0043$) and the TcdA$^-$ TcdB$^-$ mutant ($P = 0.0022$) in the Monash model of CDI and in the TcdA$^+$ TcdB$^-$ mutant-infected mice ($P < 0.0001$) in the Sanger model of CDI. Histopathological scoring of tissues from CDT$^-$ strain-infected mice resembled the results for wild-type strain-infected mice (Fig. 2B and C).

C. difficile infection can cause multiple organ dysfunction syndrome (MODS) (17, 18), but the role of toxins is unknown. Organs were therefore collected from Monash CDI model mice and their histopathology examined; 88% of wild-type strain-infected and 80% of TcdA$^-$ TcdB$^+$ strain-infected mice had damage to the thymus, sagittal lymph nodes, spleen, or kidneys (Fig. 3A). No organ damage was detected in mice infected with the TcdA$^+$ TcdB$^-$ or TcdA$^-$ TcdB$^-$ strain or mock-infected mice (Fig. 3A). To determine whether an increased amount of TcdA could elicit systemic effects similar to those observed with TcdB-producing strains, mice infected with a 500-fold higher infectious dose of the TcdA$^+$ TcdB$^-$ strain were also examined; however, no organ damage was detected (see Fig. S5C in the supplemental material). Infection with TcdB-producing strains was particularly devastating to the thymus, as evidenced by a complete loss of medullary and cortical junctions and widespread lymphocyte apoptosis (Fig. 3B). In severe cases, there were also signs of lymphoid necrosis (lymphorrexhis) found outside the secondary follicles and associated with phagocytic macrophages. Similarly, in wild-type strain- and TcdA$^-$ TcdB$^+$ strain-infected mice, sagittal lymph nodes showed a reactive phenotype categorized by the presence of lymphocytic apoptosis, areas of lymphoid depletion, and focal regions of macrophage aggregates and multinucleated giant cells, as well as a decrease in the number and size of lymphoid follicles and a marked absence of germinal centers (Fig. 3B). Mild lymphocyte apoptosis was also observed in splenic tissue isolated from mice infected with the wild type and the TcdA$^-$ TcdB$^+$ mutant (Fig. 3B), with focal areas of tissue showing loss of red and white pulp morphology, as well as an increase in tingible body macrophages and periarteriolar lymphoid sheaths (PALS). Kidney damage was only seen in wild type-infected mice, where capsular lesions were observed.

Infection with *C. difficile* toxin gene mutants elicits unique host response signatures. To further explore the effects of TcdA and TcdB on the host, we studied the immune response transcriptomic signatures seen in the large intestinal tissues collected from Monash and Sanger wild-type, TcdA$^-$ TcdB$^+$, and TcdA$^+$ TcdB$^-$ strain- and mock-infected mice (see Table S2 in the supplemental material). Tissues collected from CDT$^-$ strain-infected mice were not included in this analysis, since CDT appears to have little effect on virulence under the conditions tested in this study. Hierarchical clustering of samples showed that most TcdA$^-$ TcdB$^+$ strain-infected tissues displayed expression profiles similar to those of wild-type strain-infected tissues, whereas TcdA$^+$ TcdB$^-$ strain-infected samples clustered closely with mock-infected tissues, consistent with the attenuated virulence phenotype of the TcdA$^+$ TcdB$^-$ strains (Fig. 4). Infection with TcdB-producing strains (wild-type and TcdA$^-$ TcdB$^+$ strains) induced expression changes in a diverse group of host genes involved in the innate immune response, inflammation, and cellular apoptosis. These included *s100a8*, *lcn2*, *cxcl1*, *il1b*, and *duox2*, which encode the S100 calcium binding protein, lipocalin 2, chemokine ligand 1, interleukin 1β, and dual oxidase 2, respectively. In the absence of TcdB, these genes did not appear to be differentially regulated. Importantly, however, the expression of many of these genes was higher following infection with the wild-type strain than with the TcdA$^-$ TcdB$^+$ mutant, suggesting that TcdA, as well as TcdB, is involved in modulating the host innate immune and inflammatory response to *C. difficile* infection. Many genes involved in cellular metabolism were also differentially regulated in response to CDI, including genes encoding enzymes such as synthases, methyltransferases, oxidases, carboxypeptidases, and dehydrogenases. In addition, a profound effect on cellular detoxification pathways was noted, with a number of UDP-glucuronosyltransferase genes (*ugt1a6b*, *ugt1a6a*, *ugt1a1*, *ugt1a7c*, *ugt1a10*, *ugt2b36*, and *ugt2b35*), cytochrome P450 family protein-encoding genes (*cyp2c55*, *cyp2c65*, *cyp4b1*, *cyp4f14*, *cyp2d12*, *cyp3a13*, *cyp2d22*, and *cyp2d26*), and carboxylesterase genes (*ces1f*, *ces2*, *ces1d*, and *ces2e*) significantly downregulated. Although unrelated, these protein families play a key role in protecting host cells from damage caused by endogenous and exogenous toxins, as well as being involved in the removal of xenobiotic substances (19–21). Finally,

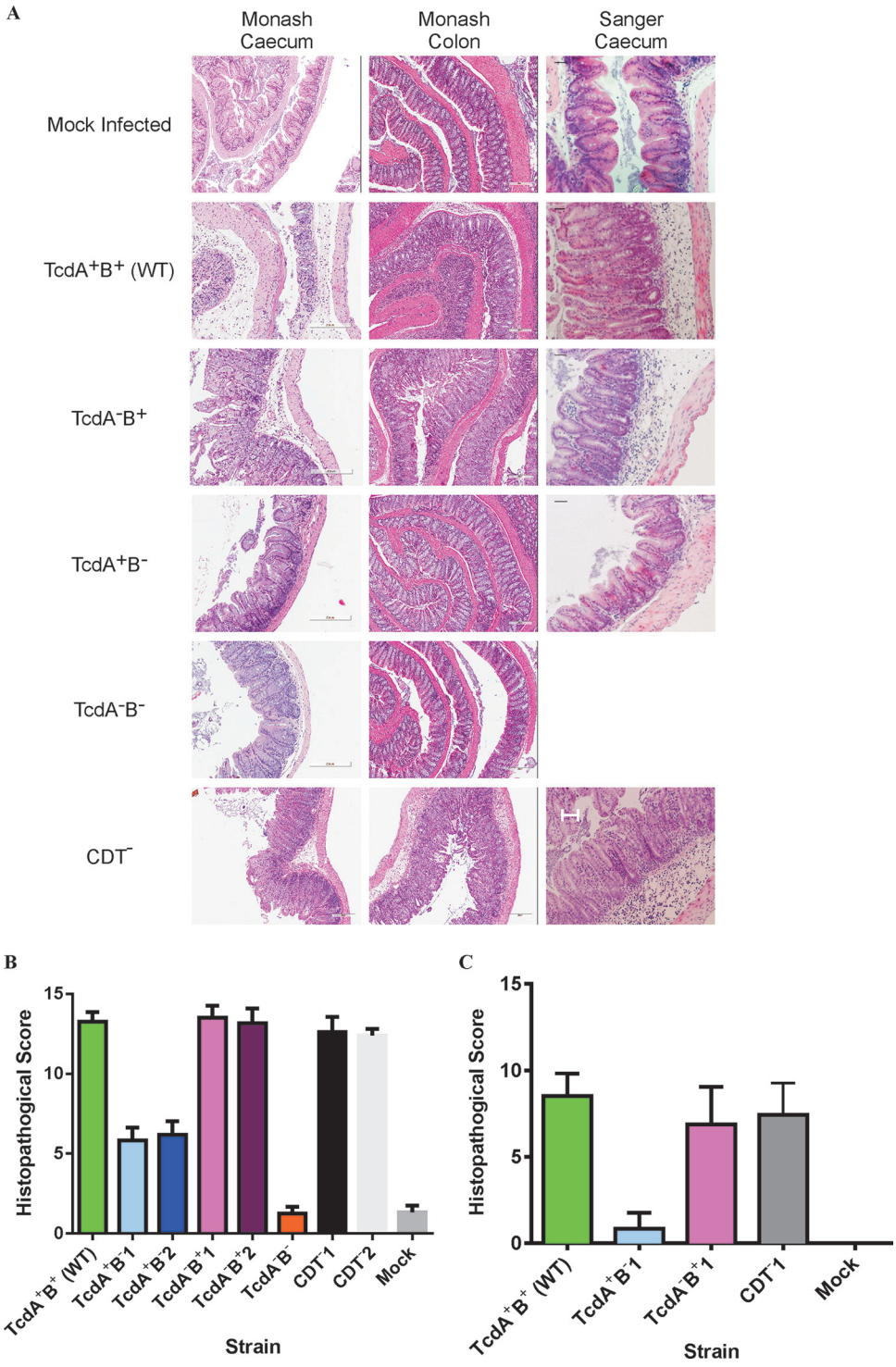

FIG 2 Toxin B causes severe local histopathological damage. Histopathological analyses of tissues collected from mice infected with the wild-type strain M7404 [TcdA$^+$B$^+$ (WT)], *tcdA* mutant 1 (TcdA$^-$B$^+$), *tcdB* mutant 1 (TcdA$^+$B$^-$), *tcdA tcdB* double mutant (TcdA$^-$B$^-$), or *cdtA* mutant 1 (CDT$^-$1) or mock infected with PBS were performed. (A) Representative images of hematoxylin-and-eosin-stained tissues from Monash mice on day 2 postinfection and from Sanger mice on day 4 postinfection are shown. Scale bars are shown (200 μm). (B) Histopathological scoring of damage to tissues from Monash mice infected with the wild-type and mutant *C. difficile* strains. Scores are shown for tissues from mice infected with the TcdA$^+$ TcdB$^+$ (WT) strain ($n = 12$), TcdA$^+$ TcdB$^-$ mutant 1 ($n = 6$), TcdA$^+$ TcdB$^-$ mutant 2 ($n = 5$), TcdA$^-$ TcdB$^+$ mutant 1 ($n = 6$), TcdA$^-$ TcdB$^+$ mutant 2 ($n = 6$), TcdA$^-$ TcdB$^-$ double mutant ($n = 6$), CDT$^-$ mutant 1 ($n = 5$), and CDT$^-$ mutant 2 ($n = 5$) and from mock-infected mice ($n = 6$). All values are mean results ± SD. (C) Histopathological scoring of damage to tissues in Sanger mice infected with wild-type and mutant *C. difficile* strains. Scores are shown for tissues from mice infected with the TcdA$^+$ TcdB$^+$ (WT) strain ($n = 12$), TcdA$^+$ TcdB$^-$ mutant 1 ($n = 12$), TcdA$^-$ TcdB$^+$ mutant 1 ($n = 8$), and CDT$^-$ mutant 1 ($n = 12$) and from mock-infected mice ($n = 12$). All values are mean results ± SD.

A

Strain	No.of mice	Organs affected				% Mice affected
		Kidney	Thymus	Spleen	SG Lns	
$TcdA^+B^+$(WT)	9	2/9	8/9	0/9	3/9	8/9**(88%)**
$TcdA^-B^+$	10	0/10	8/10	4/10	4/10	8/10**(80%)**
$TcdA^+B^-$	9	0/9	0/9	0/9	0/9	0/9**(0%)**
$TcdA^-B^-$	5	0/5	0/5	0/5	0/5	0/5**(0%)**
Mock	5	0/5	0/5	0/5	0/5	0/5**(0%)**

B

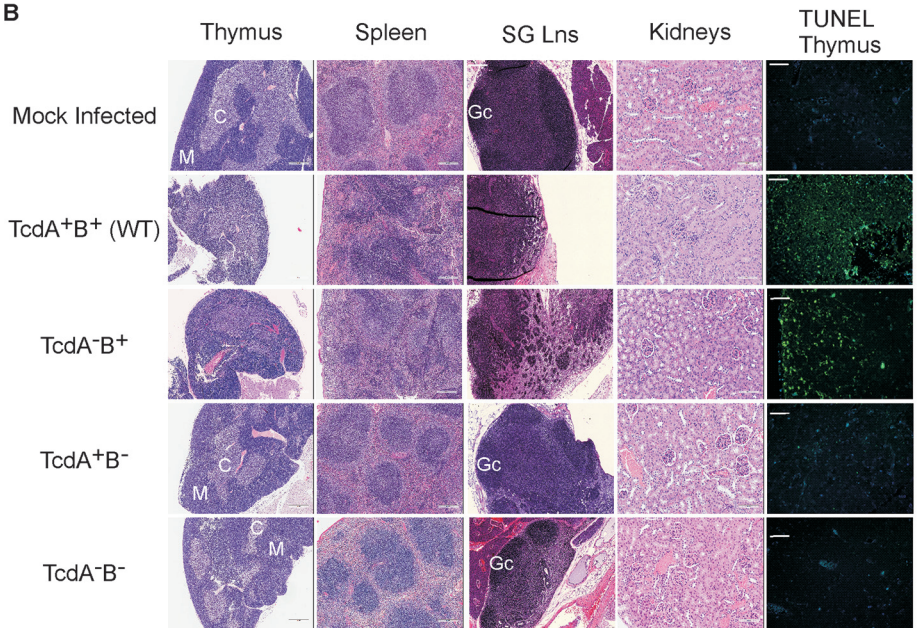

FIG 3 *C. difficile* infection with TcdB-producing strains is associated with multiorgan damage. (A) Organs were collected from Monash mice and assessed for damage compared to the state of control tissues, and the data collated. (B) Representative images of organ tissues collected from Monash CDI mice infected with wild-type strain M7404 [$TcdA^+B^+$ (WT)], *tcdA* mutant 1 ($TcdA^-B^+$), *tcdB* mutant 1 ($TcdA^+B^-$), or *tcdA tcdB* double mutant ($TcdA^-B^-$) or mock infected with PBS. Note the loss of structure in medullary and cortical regions in the thymus (M, medulla, C, cortex) and in the germinal centers (Gc) of the sagittal lymph nodes (SG Lns). Scale bars are shown (thymus, 500 μm; spleen, 200 μm; SG Lns and kidney, 100 μm).

several genes encoding solute carrier (SLC) family proteins (*slc37a1*, *slc26a3*, *slc17a4*, *slc39a5*, *slc30a10*, *slc26a2*, *slc40a1*, *slc16a5*, *slc9a2*, *slc02b1*, *slc16a9*, and *slc5a6*) were also found to be downregulated, predominantly in response to infection with the wild-type strain and the $TcdA^-$ $TcdB^+$ mutant. These proteins play a key role in many central metabolic cellular processes since they are involved in the transport of a variety of substrates, such as sugars, inorganic ions, nucleotides, and amino acids (22). Collectively, these data highlight the profound effect that *C. difficile* infections have on central processes within host epithelial cells, particularly in response to TcdB. Furthermore, unique signatures of the host response to each toxin mutant strain were identified, suggesting that clinical *C. difficile* strains might elicit differential host responses depending on the combination of toxins produced by the infecting strain.

DISCUSSION

Over the last 30 years, most studies defining the roles played by the *C. difficile* major toxins in disease utilized purified TcdA or TcdB and their direct administration to animals or application to cell lines, which provided invaluable insights into the mechanism of action of each of the toxins. It has only been in the last decade, however, that genetic manipulation technology has allowed toxin gene mutants to be constructed, facilitating hamster infection studies that have allowed the roles of the toxins to be more accurately defined (8, 9, 23). These infection studies all suggested that TcdB plays a more important role in disease than suggested by the earlier work involving purified toxins (8–10, 24). The study presented here has further defined the roles of TcdA and TcdB and has also assessed the role of CDT binary toxin in CDI, using three different animal models of disease. This work comprehensively shows that both TcdA and TcdB play a role in disease pathogenesis but that TcdB is the major virulence factor and causes severe host damage and disease in all animal models. In contrast, the CDT binary toxin appears to play a minor role in CDI under the experimental conditions used in this study, although other studies have suggested that this toxin can enhance colonization (25) or cause tissue damage in a small number of animals in a hamster CDI model (10). It is clear from this and other studies that CDT is not a major virulence factor, with a minority of virulent strains producing this toxin (13). Furthermore, a previous study has shown that TcdA- and TcdB-negative but CDT-positive strains are avirulent in the hamster infection model (26). The design of future experiments to clarify the role of CDT during infection will need to be carefully considered, since they will need to capture the subtle and synergistic effects that this toxin is likely

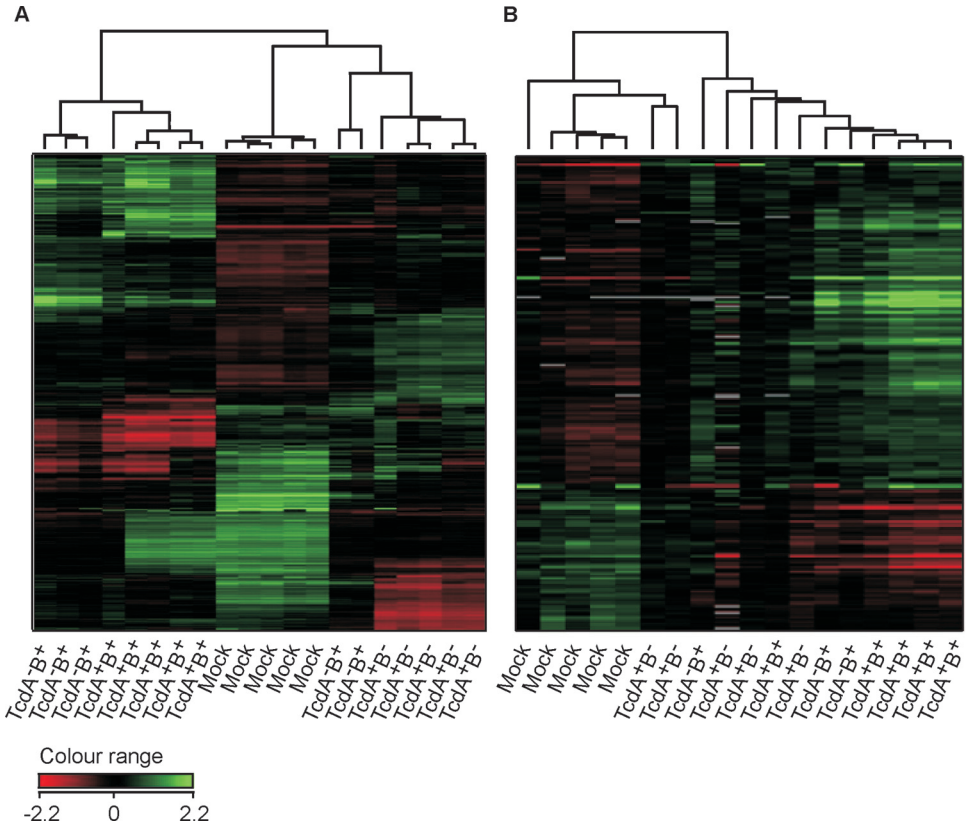

FIG 4 Transcriptomic analysis of the host response during *C. difficile* infection. Heat maps of the transcriptomes of colonic tissues collected from mice following infection with the wild-type strain M7404 [TcdA$^+$B$^+$ (WT)], *tcdB* mutant 1 (TcdA$^+$B$^-$), or *tcdA* mutant 1 (TcdA$^-$B$^+$) or mock infection with PBS using the Monash mouse model (A) or the Sanger mouse model (B) of CDI. Scaled expression values within the heat maps are color coded according to the color range shown, with red being the lowest and green being the highest level of transcription. The dendrogram shown above each heat map depicts hierarchical clustering of the transcriptomic response of each mouse following infection and was derived using a Pearson hierarchical-clustering algorithm. The infecting strains are indicated underneath the individual heat maps.

to be exerting on the host. At this time, however, the role of CDT in *C. difficile* infection and disease pathogenesis remains undefined.

Although many of the recent infection studies have unquestionably clarified the role of TcdB in CDI and showed that TcdB function does not depend on the presence of TcdA, the role of TcdA itself is less apparent (8–10, 24). Here, we clearly show in all three infection models that TcdA plays a less important role than TcdB in CDI caused by BI/NAP1/027 *C. difficile* isolates. Histopathological analysis of cecal and colonic tissues collected from infected mice showed that TcdB was responsible for the majority of intestinal damage arising during infection, with TcdA causing more superficial and localized damage. This finding contrasts with previous suggestions that TcdA is the primary cause of damage to the colonic niche during the course of a *C. difficile* infection (8), although it agrees with other research that showed that TcdB is a more potent enterotoxin than TcdA in human intestinal explants (27). Unexpectedly, this work has also identified a role for TcdA in modulating the severe effects of TcdB in the Sanger murine CDI model. Using this model, mice infected with the TcdA$^-$ TcdB$^+$ strain succumbed to infection, while those infected with the wild-type or the TcdA$^+$ TcdB$^-$ mutant strain did not. This observation aligns with previous clinical observations suggesting that naturally occurring TcdA$^-$ TcdB$^+$ strains are capable of causing more severe disease than some TcdA$^+$ TcdB$^+$ strains (5). Furthermore, a recent study showed that the administration of TcdA neutralizing antibodies in piglets with CDI resulted in more severe disease than in untreated animals (28). While further work is needed to determine the mechanism by which TcdA modulates the effects of TcdB, the simplest explanation may be one of competition: TcdA intoxication of cells may prevent TcdB from acting on the same cells, thereby limiting the pool of cells on which TcdB can act and consequently reducing disease severity. Regardless, these observations have important implications for the development of next-generation, nonantibiotic, toxin-directed CDI therapeutics, because they suggest that these approaches should focus on both TcdA and TcdB or TcdB alone since targeting only TcdA may return adverse clinical outcomes. The increasing isolation of clinical and veterinary TcdA$^-$ TcdB$^+$ variants also reinforces the need for the development of TcdB-based therapies.

The severity of disease caused by TcdB-producing strains may result from the extraintestinal organ damage that is caused by infection with these strains. These systemic effects were absent in mice challenged with *C. difficile* strains that did not produce TcdB. These observations align with previous findings showing that TcdB is cardiotoxic in a zebrafish embryo model of intoxication (29) and a study showing that the administration of TcdB-specific antibodies lessened the systemic effects of CDI in a piglet infection

model (28). Furthermore, another study showed that both TcdA and TcdB could disseminate from the gut during infection with a strain that produced both toxins, leading to systemic toxemia (18). Our results suggest that TcdB is the factor responsible for systemic dissemination and damage and may therefore be responsible for the onset of MODS, a severe complication of CDI that is associated with high mortality rates. Although this study cannot discern whether extraintestinal damage is directly mediated by TcdB or is a consequence of toxin-induced "leaky gut" that compromises gut integrity and allows the systemic dispersal of microbial components (30), including other toxins, it is clear that TcdB alone is associated with systemic and severe disease.

The systemic effects of infection with TcdB-producing *C. difficile* strains extended to many organs, including lymphoid tissues and, in particular, the thymus. Thymic injury during infection with other pathogens has been described (14–16) and can be associated with poor outcomes postrecovery (31). Thymic atrophy associated with infectious diseases can result in temporary lymphocyte depletion and altered circulating T-cell populations, which is of little consequence in healthy individuals where the thymus and immune functions are restored rapidly following infection. However, age-related thymic involution can result in an inability to restore immune function following infection (31). CDI effects on the thymus may influence immune function postinfection in a similar way, resulting in an increased risk of disease relapse or secondary infections, such as funguria or vancomycin-resistant *Enterococcus* (VRE) infections, which are associated with CDI patients (32, 33). This finding is particularly relevant to elderly patients, a group at significant risk for CDI (34) who have already undergone thymic atrophy (31).

Transcriptomic analysis of mice infected with the wild-type and mutant strains revealed that TcdB is the major factor inducing host innate immune and proinflammatory responses. These responses were generally stronger in mice infected with the wild-type strain than in those infected with the $TcdA^-$ $TcdB^+$ derivative, suggesting that TcdA also plays a role in upregulating these responses, which agrees with similar studies using purified toxins (35, 36). Of note, TcdB was recently shown to induce cellular apoptosis via NADPH oxidase-mediated production of reactive superoxide species, and a reduction in reactive oxygen species (ROS) activity protected colonic explants from TcdB-induced damage (37). Although upregulation of NADPH oxidase genes was not detected in our study, one of the most upregulated pathways following infection was found to be Duox2, which produces ROS in a way similar to NADPH oxidase. Duox2 is predominantly expressed in gastrointestinal epithelial cells, where it plays an important role in host defense against invading pathogens, such as *Listeria monocytogenes*, *Salmonella enterica* serovar Typhimurium, and *Helicobacter* spp., through the inducible production of hydrogen peroxide and ROS (38). As with NADPH oxidase (37), it appears that TcdB might induce aberrant activation of the Duox2 pathway within the intestinal epithelium during infection. Since ROS is known to cause organ damage and is also implicated in the pathogenesis of gastrointestinal conditions, such as small intestine ischemia and ulcerative colitis (39–41), it is possible that the uncontrolled Duox2-mediated burst of H_2O_2 and ROS resulting from *C. difficile* infection with TcdB-producing strains contributes to gut damage. Although further work is needed to understand the role that upregulation of Duox2 may play in *C. difficile*-induced gut damage, this pathway may represent a novel therapeutic target for reducing the level of gastrointestinal damage during CDI by reducing ROS production. Similar approaches have been used to develop a promising class of novel therapeutics that inhibit NADPH oxidases for the treatment of numerous inflammatory diseases and cancers (42, 43).

Overall, our results have important implications for the development and validation of treatment agents for CDI and for disease pathogenesis studies. Genetically, *C. difficile* is a heterogeneous species, with new disease-causing variants emerging regularly. Although many cases of CDI are acquired within hospitals, recent molecular epidemiological studies have shown that many other environmental sources may contribute to the infection reservoir. Regardless of the environmental source, TcdB appears to be the only toxin common to all current and emerging human and animal disease-causing isolates (44–46), reinforcing the outcomes presented here and the need for TcdB-targeted therapeutics. Our results also support the use of multiple animal infection models for the purpose of comprehensive evaluation of therapeutics. Finally, despite being an infection that is confined to the gut, *C. difficile* infection is clearly shown by this work to cause damage to organs distal to the infection site, and this work also provides new insights into the systemic host damage that can occur as a consequence of a localized gastrointestinal infection.

MATERIALS AND METHODS

Construction and characterization of toxin gene mutants. The *tcdA*, *tcdB*, and *tcdAB C. difficile* mutants were made using targetron technology and utilizing appropriately retargeted derivatives of plasmid pDLL1 and conjugative matings from a *B. subtilis* BS34A donor strain, as previously described (23). For isolation of the double toxin mutant, antibiotic selection could not be used, and so this strain was detected by PCR screening for both the *tcdA*- and *tcdB*-specific insertion of the targetron. The targetron element inserted after nucleotide 4068 of the sense strand for *tcdA*, nucleotide 1587 of the sense strand for *tcdB*, and nucleotide 421 of the sense strand for *cdtA*. The *tcdAB* double toxin mutant was constructed using *tcdB* mutant 1 as the parent strain. To verify that the targetron insertions had occurred as anticipated, PCR using the following oligonucleotide primers were used: for *tcdA*, EBS-universal (sigma) and JRP3602 (TAAATGTACTACCTACAATAACAGAGGG); for *tcdB*, EBS-universal and JRP1592 (GTGGCCCTGAAGCATATG); and for *cdtA*, EBS-universal and JRP1744 (GGGAAAGAAAAGAAGCAGAAAG). Strain numbers were assigned as follows: for *tcdA* mutant 1, DLL3043; for *tcdA* mutant 2, DLL3045; for *tcdB* mutant 1, DLL3101; for *tcdB* mutant 2, DLL3102; and for the *tcdAB* mutant, DLL3121.

Each mutant was also confirmed by Southern hybridization analysis as described previously, using an *ermB*-specific PCR product (47), a *tcdB*- or *tcdA*-specific PCR product (9), or a *cdt*-specific PCR product amplified using primers JRP1746 (GGAAGACGAAGATTTGGATACA) and JRP2505 (GGTTTTAGCTCAGACATAGGGA).

To confirm the correct toxin production profiles in each mutant and wild-type strain, TcdA-, TcdB-, and CdtA-specific Western blot analyses were performed as described previously (9, 13), except that toxins were precipitated from culture supernatants using chloroform-methanol (8), and Vero and HT29 cell cytotoxicity and neutralization assays were also performed as described previously (9).

Complementation of the *tcdA* and *tcdB* genes was attempted; however, despite multiple attempts, it did not prove possible to clone the intact *tcdA* or *tcdB* gene into an appropriate shuttle plasmid that would facilitate conjugative transfer into *C. difficile*.

Animal infection trials. Virulence trials using the Monash and Sanger mouse models and the Hines hamster model were performed as described previously (2) and are described in detail in the supplemental material. For the Monash mouse model, all monitoring was carried out in accor-

dance with Victorian State Government regulations and the Monash University Animal Ethics guidelines. All experiments were approved by the Monash University SOBS B Animal Ethics Committee. All Sanger mouse model experiments were performed in accordance with the United Kingdom Home Office Animals (Scientific Procedures) Act of 1986. All hamster experiments were approved by the Institutional Animal Care and Use Committee (IACUC) at the Hines VA Hospital.

Histopathological scoring and staining. All histopathological analysis was performed by an independent, certified pathologist at the Australian Phenomics Network, University of Melbourne. Monash and Sanger colonic and cecal sections were assessed using a scoring system based on previously established parameters (26), described in detail in Table S3 in the supplemental material. Terminal deoxynucleotidyltransferase-mediated dUTP-biotin nick end labeling (TUNEL) staining was performed on thymus sections using an *in situ* cell death detection kit with fluorescein (Roche), following the manufacturer's instructions.

Microarrays. Total RNA was extracted from colonic tissues isolated from mice at Monash University and the terminal cecal tissues of mice from the Sanger Institute, using the Qiagen RNeasy kit according to the manufacturer's instructions. RNA quality was assessed using the Agilent 2100 bioanalyzer (Agilent Technologies), and microarray gene expression analyses performed on an Illumina GEX platform. Microarray data were analyzed using GeneSpring software (Agilent Technologies). Genes showing differential expression were selected with a Benjamini-Hochberg-corrected P value of <0.05 and fold change (compared to mock-infected controls) of >2 for Monash tissues or >1.5 for Sanger tissues. The transcriptomic responses of samples were arranged as a heat map (Fig. 4) by applying a Pearson hierarchical-clustering algorithm based on both entities and conditions. Analyses of enriched Gene Ontology terms and KEGG pathways associated with differentially expressed gene sets were subsequently performed using the DAVID (Database for Annotation, Visualisation and Integrated Discovery) (27) functional classification tool and the InnateDB database (28) for innate immune response.

Note that additional methods are provided in the supplemental material.

SUPPLEMENTAL MATERIAL

Supplemental material for this article may be found at http://mbio.asm.org/lookup/suppl/doi:10.1128/mBio.00551-15/-/DCSupplemental.

Text S1, DOC file, 0.1 MB.
Figure S1, JPG file, 0.3 MB.
Figure S2, JPG file, 0.3 MB.
Figure S3, JPG file, 0.6 MB.
Figure S4, JPG file, 0.8 MB.
Figure S5, JPG file, 1.5 MB.
Figure S6, JPG file, 0.8 MB.
Table S1, DOC file, 0.03 MB.
Table S2, XLSX file, 0.1 MB.
Table S3, DOC file, 0.04 MB.

ACKNOWLEDGMENTS

Research at Monash University was supported by Project grants 545858 and APP1051584 (Australian National Health and Medical Research Council) and Discovery grant DP1093891 (Australian Research Council). D.L. was supported by Future fellowship FT120100779 (Australian Research Council). Research at the Sanger Institute was funded by the Wellcome Trust (grants 098051 and 086418) and the Medical Research Council New Investigator Research grant (grant 93614 to T.D.L.). S.J. and D.N.G. are funded by the VA Merit Review program.

We thank Tina Cardamone (Australian Phenomics Network, University of Melbourne) and John Finney and Rolfe Howlett (R & A Veterinary Pathology Services, NSW) for pathology services. We are also grateful to Mark Arends (University of Cambridge) for assisting with the histological scoring of mouse tissues from the Sanger Institute.

REFERENCES

1. **Freeman J, Bauer MP, Baines SD, Corver J, Fawley WN, Goorhuis B, Kuijper EJ, Wilcox MH.** 2010. The changing epidemiology of *Clostridium difficile* infections. Clin Microbiol Rev **23:**529–549. http://dx.doi.org/10.1128/CMR.00082-09.
2. **Squire MM, Carter GP, Mackin KE, Chakravorty A, Norén T, Elliott B, Lyras D, Riley TV.** 2013. Novel molecular type of *Clostridium difficile* in neonatal pigs, Western Australia. Emerg Infect Dis **19:**790–792. http://dx.doi.org/10.3201/eid1905.121062.
3. **Knight DR, Riley TV.** 2013. Prevalence of gastrointestinal *Clostridium difficile* carriage in Australian sheep and lambs. Appl Environ Microbiol **79:**5689–5692. http://dx.doi.org/10.1128/AEM.01888-13.
4. **Aktories K.** 2011. Bacterial protein toxins that modify host regulatory GTPases. Nat Rev Microbiol **9:**487–498. http://dx.doi.org/10.1038/nrmicro2592.
5. **Drudy D, Fanning S, Kyne L.** 2007. Toxin A-negative, toxin B-positive *Clostridium difficile*. Int J Infect Dis **11:**5–10. http://dx.doi.org/10.1016/j.ijid.2006.04.003.
6. **Gerding DN, Johnson S, Rupnik M, Aktories K.** 2014. *Clostridium difficile* binary toxin CDT: mechanism, epidemiology, and potential clinical importance. Gut Microbes **5:**15–27. http://dx.doi.org/10.4161/gmic.26854.
7. **Lyerly DM, Phelps CJ, Toth J, Wilkins TD.** 1986. Characterization of toxins A and B of *Clostridium difficile* with monoclonal antibodies. Infect Immun **54:**70–76.
8. **Kuehne SA, Cartman ST, Heap JT, Kelly ML, Cockayne A, Minton NP.** 2010. The role of toxin A and toxin B in *Clostridium difficile* infection. Nature **467:**711–713. http://dx.doi.org/10.1038/nature09397.
9. **Lyras D, O'Connor JR, Howarth PM, Sambol SP, Carter GP, Phumoonna T, Poon R, Adams V, Vedantam G, Johnson S, Gerding DN, Rood JI.** 2009. Toxin B is essential for virulence of *Clostridium difficile*. Nature **458:**1176–1179. http://dx.doi.org/10.1038/nature07822.
10. **Kuehne SA, Collery MM, Kelly ML, Cartman ST, Cockayne A, Minton NP.** 2014. Importance of toxin A, toxin B, and CDT in virulence of an epidemic *Clostridium difficile* strain. J Infect Dis **209:**83–86. http://dx.doi.org/10.1093/infdis/jit426.
11. **Gill N, Finlay BB.** 2011. The gut microbiota: challenging immunology. Nat Rev Immunol **11:**636–637. http://dx.doi.org/10.1038/nri3061.
12. **Ballard JD.** 2010. Medical microbiology: a toxin contest. Nature **467:**665–666. http://dx.doi.org/10.1038/467665a.
13. **Carter GP, Lyras D, Allen DL, Mackin KE, Howarth PM, O'Connor JR, Rood JI.** 2007. Binary toxin production in *Clostridium difficile* is regulated by CdtR, a LytTR family response regulator. J Bacteriol **189:**7290–7301. http://dx.doi.org/10.1128/JB.00731-07.
14. **Chen X, Katchar K, Goldsmith JD, Nanthakumar N, Cheknis A, Gerding DN, Kelly CP.** 2008. A mouse model of *Clostridium difficile*-associated disease. Gastroenterology **135:**1984–1992. http://dx.doi.org/10.1053/j.gastro.2008.09.002.
15. **Okayasu I, Hatakeyama S, Yamada M, Ohkusa T, Inagaki Y, Nakaya R.** 1990. A novel method in the induction of reliable experimental acute and chronic ulcerative colitis in mice. Gastroenterology **98:**694–702.
16. **Lawley TD, Clare S, Walker AW, Goulding D, Stabler RA, Croucher N, Mastroeni P, Scott P, Raisen C, Mottram L, Fairweather NF, Wren BW, Parkhill J, Dougan G.** 2009. Antibiotic treatment of *Clostridium difficile* carrier mice triggers a supershedder state, spore-mediated transmission, and severe disease in immunocompromised hosts. Infect Immun **77:**3661–3669. http://dx.doi.org/10.1128/IAI.00558-09.
17. **Dobson G, Hickey C, Trinder J.** 2003. *Clostridium difficile* colitis causing toxic megacolon, severe sepsis and multiple organ dysfunction syndrome. Intensive Care Med **29:**1030. http://dx.doi.org/10.1007/s00134-003-1754-7.
18. **Steele J, Chen K, Sun X, Zhang Y, Wang H, Tzipori S, Feng H.** 2012. Systemic dissemination of *Clostridium difficile* toxins A and B is associated with severe, fatal disease in animal models. J Infect Dis **205:**384–391. http://dx.doi.org/10.1093/infdis/jir748.
19. **Guengerich FP.** 2008. Cytochrome P450 and chemical toxicology. Chem Res Toxicol **21:**70–83. http://dx.doi.org/10.1021/tx700079z.
20. **Rowland A, Miners JO, Mackenzie PI.** 2013. The UDP-glucuronosyltransferases: their role in drug metabolism and detoxification. Int J Biochem Cell Biol **45:**1121–1132. http://dx.doi.org/10.1016/j.biocel.2013.02.019.
21. **Zhuang XM, Wei X, Tan Y, Xiao WB, Yang HY, Xie JW, Lu C, Li H.**

2014. Contribution of carboxylesterase and cytochrome P450 to the bioactivation and detoxification of isocarbophos and its enantiomers in human liver microsomes. Toxicol Sci **140:**40–48. http://dx.doi.org/10.1093/toxsci/kfu067.

22. **Hediger MA, Romero MF, Peng JB, Rolfs A, Takanaga H, Bruford EA.** 2004. The ABCs of solute carriers: physiological, pathological and therapeutic implications of human membrane transport proteins. Pflugers Arch **447:**465–468. http://dx.doi.org/10.1007/s00424-003-1192-y.
23. **O'Connor JR, Lyras D, Farrow KA, Adams V, Powell DR, Hinds J, Cheung JK, Rood JI.** 2006. Construction and analysis of chromosomal *Clostridium difficile* mutants. Mol Microbiol **61:**1335–1351. http://dx.doi.org/10.1111/j.1365-2958.2006.05315.x.
24. **Li S, Shi L, Yang Z, Zhang Y, Perez-Cordon G, Huang T, Ramsey J, Oezguen N, Savidge TC, Feng H.** 2015. Critical roles of *Clostridium difficile* toxin B enzymatic activities in pathogenesis. Infect Immun **83:**502–513. http://dx.doi.org/10.1128/IAI.02316-14.
25. **Schwan C, Stecher B, Tzivelekidis T, van Ham M, Rohde M, Hardt WD, Wehland J, Aktories K.** 2009. *Clostridium difficile* toxin CDT induces formation of microtubule-based protrusions and increases adherence of bacteria. PLoS Pathog **5:**e1000626. http://dx.doi.org/10.1371/journal.ppat.1000626.
26. **Geric B, Carman RJ, Rupnik M, Genheimer CW, Sambol SP, Lyerly DM, Gerding DN, Johnson S.** 2006. Binary toxin-producing, large clostridial toxin-negative *Clostridium difficile* strains are enterotoxic but do not cause disease in hamsters. J Infect Dis **193:**1143–1150. http://dx.doi.org/10.1086/501368.
27. **Savidge TC, Pan WH, Newman P, O'Brien M, Anton PM, Pothoulakis C.** 2003. *Clostridium difficile* toxin B is an inflammatory enterotoxin in human intestine. Gastroenterology **125:**413–420. http://dx.doi.org/10.1016/S0016-5085(03)00902-8.
28. **Steele J, Mukherjee J, Parry N, Tzipori S.** 2013. Antibody against TcdB, but not TcdA, prevents development of gastrointestinal and systemic *Clostridium difficile* disease. J Infect Dis **207:**323–330. http://dx.doi.org/10.1093/infdis/jis669.
29. **Hamm EE, Voth DE, Ballard JD.** 2006. Identification of *Clostridium difficile* toxin B cardiotoxicity using a zebrafish embryo model of intoxication. Proc Natl Acad Sci U S A **103:**14176–14181. http://dx.doi.org/10.1073/pnas.0604725103.
30. **Brenchley JM, Price DA, Schacker TW, Asher TE, Silvestri G, Rao S, Kazzaz Z, Bornstein E, Lambotte O, Altmann D, Blazar BR, Rodriguez B, Teixeira-Johnson L, Landay A, Martin JN, Hecht FM, Picker LJ, Lederman MM, Deeks SG, Douek DC.** 2006. Microbial translocation is a cause of systemic immune activation in chronic HIV infection. Nat Med **12:**1365–1371. http://dx.doi.org/10.1038/nm1511.
31. **Calder AE, Hince MN, Dudakov JA, Chidgey AP, Boyd RL.** 2011. Thymic involution: where endocrinology meets immunology. Neuroimmunomodulation **18:**281–289. http://dx.doi.org/10.1159/000329496.
32. **Poduval RD, Kamath RP, Corpuz M, Norkus EP, Pitchumoni CS.** 2000. *Clostridium difficile* and vancomycin-resistant *Enterococcus*: the new nosocomial alliance. Am J Gastroenterol **95:**3513–3515. http://dx.doi.org/10.1111/j.1572-0241.2000.03291.x.
33. **Fujitani S, George WL, Morgan MA, Nichols S, Murthy AR.** 2011. Implications for vancomycin-resistant *Enterococcus* colonization associated with *Clostridium difficile* infections. Am J Infect Control **39:**188–193. http://dx.doi.org/10.1016/j.ajic.2010.10.024.
34. **Vardakas KZ, Konstantelias AA, Loizidis G, Rafailidis PI, Falagas ME.** 2012. Risk factors for development of *Clostridium difficile* infection due to BI/NAP1/027 strain: a meta-analysis. Int J Infect Dis **16:**e768–e773. http://dx.doi.org/10.1016/j.ijid.2012.07.010.
35. **D'Auria KM, Kolling GL, Donato GM, Warren CA, Gray MC, Hewlett EL, Papin JA.** 2013. In vivo physiological and transcriptional profiling reveals host responses to *Clostridium difficile* toxin A and toxin B. Infect Immun **81:**3814–3824. http://dx.doi.org/10.1128/IAI.00869-13.
36. **Hirota SA, Iablokov V, Tulk SE, Schenck LP, Becker H, Nguyen J, Al Bashir S, Dingle TC, Laing A, Liu J, Li Y, Bolstad J, Mulvey GL, Armstrong GD, MacNaughton WK, Muruve DA, MacDonald JA, Beck PL.** 2012. Intrarectal instillation of *Clostridium difficile* toxin A triggers colonic inflammation and tissue damage: development of a novel and efficient mouse model of *Clostridium difficile* toxin exposure. Infect Immun **80:**4474–4484. http://dx.doi.org/10.1128/IAI.00933-12.
37. **Farrow MA, Chumbler NM, Lapierre LA, Franklin JL, Rutherford SA, Goldenring JR, Lacy DB.** 2013. *Clostridium difficile* toxin B-induced necrosis is mediated by the host epithelial cell NADPH oxidase complex. Proc Natl Acad Sci U S A **110:**18674–18679. http://dx.doi.org/10.1073/pnas.1313658110.
38. **Grasberger H, El-Zaatari M, Dang DT, Merchant JL.** 2013. Dual oxidases control release of hydrogen peroxide by the gastric epithelium to prevent *Helicobacter felis* infection and inflammation in mice. Gastroenterology **145:**1045–1054. http://dx.doi.org/10.1053/j.gastro.2013.07.011.
39. **Otamiri T, Sjödahl R.** 1991. Oxygen radicals: their role in selected gastrointestinal disorders. Dig Dis **9:**133–141. http://dx.doi.org/10.1159/000171299.
40. **Sasaki M, Joh T.** 2007. Oxidative stress and ischemia-reperfusion injury in gastrointestinal tract and antioxidant, protective agents. J Clin Biochem Nutr **40:**1–12. http://dx.doi.org/10.3164/jcbn.40.1.
41. **Kim YJ, Kim EH, Hahm KB.** 2012. Oxidative stress in inflammation-based gastrointestinal tract diseases: challenges and opportunities. J Gastroenterol Hepatol **27:**1004–1010. http://dx.doi.org/10.1111/j.1440-1746.2012.07108.x.
42. **Diebold BA, Smith SM, Li Y, Lambeth JD.** 24 March 2014. NOX2 as a target for drug development: indications, possible complications, and progress. Antioxid Redox Signal, in press. http://dx.doi.org/10.1089/ars.2014.5862.
43. **Harrison IP, Selemidis S.** 2014. Understanding the biology of reactive oxygen species and their link to cancer: Nox oxidases as novel pharmacological targets. Clin Exp Pharmacol Physiol **41:**533–542. http://dx.doi.org/10.1111/1440-1681.12238.
44. **Lim SK, Stuart RL, Mackin KE, Carter GP, Kotsanas D, Francis MJ, Easton M, Dimovski K, Elliott B, Riley TV, Hogg G, Paul E, Korman TM, Seemann T, Stinear TP, Lyras D, Jenkin GA.** 2014. Emergence of a ribotype 244 strain of *Clostridium difficile* associated with severe disease and related to the epidemic ribotype 027 strain. Clin Infect Dis **58:**1723–1730. http://dx.doi.org/10.1093/cid/ciu203.
45. **Eyre DW, Cule ML, Wilson DJ, Griffiths D, Vaughan A, O'Connor L, Ip CL, Golubchik T, Batty EM, Finney JM, Wyllie DH, Didelot X, Piazza P, Bowden R, Dingle KE, Harding RM, Crook DW, Wilcox MH, Peto TE, Walker AS.** 2013. Diverse sources of *C. difficile* infection identified on whole-genome sequencing. N Engl J Med **369:**1195–1205. http://dx.doi.org/10.1056/NEJMoa1216064.
46. **Hensgens MP, Keessen EC, Squire MM, Riley TV, Koene MG, de Boer E, Lipman LJ, Kuijper EJ, European Society of Clinical Microbiology and Infectious Diseases Study Group for *Clostridium difficile* (ESGCD).** 2012. *Clostridium difficile* infection in the community: a zoonotic disease? Clin Microbiol Infect **18:**635–645. http://dx.doi.org/10.1111/j.1469-0691.2012.03853.x.
47. **Carter GP, Awad MM, Hao Y, Thelen T, Bergin IL, Howarth PM, Seemann T, Rood JI, Aronoff DM, Lyras D.** 2011. TcsL is an essential virulence factor in *Clostridium sordellii* ATCC 9714. Infect Immun **79:**1025–1032. http://dx.doi.org/10.1128/IAI.00968-10.